Study of the collapse of granular columns using two-dimensional discrete-grain simulation

By L. STARON and E. J. HINCH

Department of Applied Mathematics and Theoretical Physics, Centre for Mathematical Sciences,
University of Cambridge, Wilberforce Road, Cambridge CB3 0WA, UK

Numerical simulations of the collapse and spreading of granular columns onto a horizontal plane using the Contact Dynamics method are presented. The results are in agreement with previous experimental work. The final shape of the deposit appears to depend only on the initial aspect ratio a of the column. The normalized runout distance has a power-law dependence on the aspect ratio a, a dependence incompatible with a simple friction model. The dynamics of the collapse is shown to be mostly controlled by a free fall of the column. Energy dissipation at the base of the column can be described simply by a coefficient of restitution. Hence the energy available for the sideways flow is proportional to the initial potential energy E_0. The dissipation process within the sideways flow is approximated well by basal friction, unlike the behaviour of the runout distance. The proportion of mass ejected sideways is shown to play a determining role in the spreading process: as a increases, the same fraction of initial potential energy E_0 drives an increasing proportion of the initial mass against friction. This gives a possible explanation for the power-law dependence of the runout distance on a. We propose a new scaling for the runout distance that matches the data well, is compatible with a friction model, and provides a qualitative explanation of the column collapse.

1. Introduction

Although they have been an important subject in recent research, granular flows remain intriguing in many aspects of their behaviour (see e.g. Rajchenbach 2000; Goldhirsch 2003). The understanding of such flows has obvious application in industrial processes, which often handle all kinds of powders and granules. But it is also crucial in the geophysical issue of catastrophic flows. Rock avalanches, landslides and pyroclastic flows all involve a granular solid phase, and can become dramatic in their behaviour. In the absence of a clear physical background for the modelling of these large-scale natural granular flows, their characterization relies mainly on the observation of the final deposits, and in particular, of the final runout distance (Iverson, Schilling & Vallance 1998; Dade & Huppert 1998). A simple effective basal friction μ_e is often advocated as the most convenient description of the dissipation process. This allows an *in-situ* quantification of the mobility of the flow, knowing the runout distance and the initial height of the material. Moreover, basal friction is easily incorporated in continuous modelling, such as shallow-water equations for instance (Savage & Hutter 1989; Mangeney-Castelneau *et al.* 2004; Kerswell 2005). However, the dependence of this effective friction on the nature of the material, on the characteristics of the collapse and on the dynamics of the flow, has yet to be found.

Systematic studies of the frictional properties and the spreading of granular flows on inclined planes have been carried out (Pouliquen 1999; Pouliquen & Forterre 2002). However, until recently, the simple case of a granular mass collapsing onto a horizontal plane had not been addressed. Experiments have now investigated this problem, and studied the collapse and spreading of a suddenly released column of grains onto a horizontal plane (Lube *et al.* 2004; Lajeunesse, Mangeney-Castelneau & Vilotte 2004; Balmforth & Kerswell 2005). Essentially, the effect of the initial geometry of the column on the geometry of the final deposit has been studied. The main result consists of scaling laws for the runout distance. In particular, when the initial aspect ratio of the collapsing column is large enough, the runout distance normalized by the initial radius of the column shows a power-law dependence on the initial aspect ratio. Moreover, this dependence varies with the conditions of the experiment, in particular between axisymmetric and quasi-two-dimensional configurations. Although simple models relying on a Coulomb-failure analysis or a shallow-water approximation for the flow have been proposed, no clear physical understanding of the granular collapse process has yet been achieved. In particular, the scaling laws obtained for the runout distance are incompatible with a simple basal friction model, and this brings into question the mode of energy dissipation occurring in the successive steps of the collapse dynamics.

In this context, the use of computer simulations to reproduce numerically the collapse of a granular column is expected to give interesting new insights into the problem. Discrete element methods allow the simulation of each grain forming the granular mass, giving access to each grain's trajectory. We can thus hope to access a picture of the collapse phenomena that would be otherwise very difficult to obtain in experiments. The aim of the present work is to determine the mechanisms controlling the spreading dynamics: fall of the column, dissipation at the base, ejection of mass sideways and dissipation in the outflow. Therefore, we have applied the Contact Dynamics algorithm (Moreau 1994; Jean 1994) in two dimensions. The numerical procedures are explained in §2. A similar numerical method has been used recently by Zenit (2005). After briefly recalling and commenting on the experimental results obtained by other authors (Lube *et al.* 2004; Lajeunesse *et al.* 2004; Balmforth & Kerswell 2005) in §3, the different regimes of spreading are qualitatively described and scaling laws are established in §4. We observe a very good agreement between the experiments and the simulations. Details of the dynamics of the vertical fall and of the sideways spreading are presented in §5. The dissipation of energy and the transfer of energy from vertical fall to horizontal motion are examined in §6. We show that the energy available for the spreading is simply proportional to the initial potential energy of the column and that basal friction is a very good approximation for the dissipation within the sideways flow. We conclude that the ability of the column to eject the grains sideways is a major factor in the dynamics. This leads us to question the scaling laws obtained for the runout distance as perhaps fortuitous and corresponding to a transient regime. A new empirical fit, compatible with a friction law, and qualitatively describing the collapse phenomenology, is proposed in §7. A summary of the results and further discussion are given in §8.

2. Numerical procedures

2.1. *Simulation method*

The numerical methods used for the simulation of granular material are known under the generic name of discrete element methods (DEM). They take into account the

individual existence of each discrete grain forming the medium, and usually neglect the role of the interstitial fluid filling the space between the grains. Such an approximation makes these methods appropriate for the modelling of dry granular matter. In the absence of any influence of the interstitial fluid (air in the present case), the behaviour of the collection of grains is entirely driven by the standard equations of motion, and the contact laws describing the collisions between the grains.

Modelling the contact phenomena consists in finding relations between the contact force and various quantities referring to the physical and/or chemical processes taking place at the surface of the two bodies in contact. These microscopic interactions can be of different types. They can involve for instance elastic or plastic deformation of asperities, adhesion due to Van der Waals forces, ageing processes, etc. In any case, the complexity of these phenomena cannot be directly incorporated in the contact models, due to practical reasons of numerical feasibility or efficacy, and also because such complex models may not be realistic. Basically, DEM assume small elastic deformation, with possible viscous effects, and frictional dissipation as contact phenomenology (Cundall & Stack 1979).

It is beyond the scope of this paper to give a detailed account of the numerical method used, and further information will be found in references cited. Hence we will just specify the main hypotheses governing the behaviour of the numerical grains. In the absence of a clear physical background for modelling of contact phenomena, a possible strategy is to assume that grains are interacting only through hard-core repulsion and non-smooth Coulombic friction. This model is adopted in the Contact Dynamics (CD) algorithm (Moreau 1994; Jean 1994) that we have applied in the present work. This implies that two grains have to touch for the contact force to be non-zero, and no distant interaction is permitted. Once in contact, two grains cannot become closer, and any normal relative motion is repulsive: the grains are perfectly rigid. A microscopic coefficient of friction μ characterizes the Coulombic friction threshold $\pm\mu N$, where N is the normal force, and μ describes the frictional dissipation at grain scale. The tangential force T between two grains in contact can either be below the Coulombic friction threshold, and in that case no tangential slip motion is possible, or it can be exactly equal to the Coulombic friction threshold, and in that case slip motion will dissipate energy. These contact laws allow for *multiple collisions* between the grains, when the grains are in contact with one or more neighbours while they are undergoing collisions with others. The simple case of a binary collision must also be fully described by the algorithm: a Newtonian coefficient of restitution ρ is introduced, which gives the velocities of the grains after a collision from their velocities before the collision. This coefficient of restitution appears in the calculation of the velocity of all the grains. These contact laws are simplistic with regard to the microscopic reality of contact phenomena. Nevertheless, they are sufficient to reproduce the collective dynamics of a collection of grains.

2.2. *Numerical experiments*

Using the CD method, we have simulated two-dimensional collections of non-adhesive rigid circular grains. The diameter d of the grains is uniformly distributed in a small interval such that $d_{min}/d_{max} = 2/3$. This slight polydispersity of grain size is mainly introduced to break any crystal-like ordering of the grains which might have a non-negligible effect in two-dimensional simulations. However, the range of grain size is sufficiently narrow for the polydispersity not to produce segregation and not to affect the runout results. In the following, d denotes the mean grain diameter. The influence of the grain size was not systematically investigated here; experiments by Lajeunesse

et al. (2004) show that its role in the collapse dynamics is very weak. We have ensured that the size of the grains was small compared to the length scales of the column. The coefficient of restitution ρ for collision is the same between the grains and between the grains and the bottom plane, and was chosen $\rho = 0.5$. The microscopic coefficient of friction is the same at all contacts and set at $\mu = 1$. The values of these parameters are a reasonably good approximation to the properties of glass beads. The systematic investigation of the influence of the value of ρ and μ is beyond the scope of this paper, and will be the subject of further work. However, it can be shown that the sensitivity of the system to these values is weak, at least in the neighbourhood of the values chosen for the present work. This was also found by Zenit (2005) in the case of the coefficient of friction μ. For ρ close to 1, many particles escape through strong bouncing, which completely changes the behaviour.

The numerical experiment consists in releasing a column of grains in the gravity field onto a flat bottom plane, and studying the collapse and the resulting spreading dynamics of the granular mass. The bottom plane in our experiment is perfectly smooth. Laboratory experiments carried out on rough and smooth surfaces have shown that the general behaviour of the mass of grains (in particular the final runout distance) is not affected by the roughness of the plane, apart from a slight transformation of the deposit final shape (Lajeunesse *et al.* 2004).

The initial columns are prepared by means of a random rain of grains between two vertical walls. The compacity of the packing is $c_0 \simeq 0.82$. The dimensions of the column are its radius R_0 and its height H_0, and $a = H_0/R_0$ is the initial aspect ratio. We have considered four different values of R_0 such that $R_0/d = 10, 20, 30$ and 40, and twenty values of H_0 were used, with H_0/d varying between 50 and 175. At time $t = 0$, the vertical walls are instantaneously removed, and the column collapses due to gravity. The dimensions of the final deposit are the final runout distance R_∞, and the final height H_∞. The compacity of the final deposit is $c_\infty \simeq 0.78$, i.e. close to the initial compacity in spite of a slight loosening of the packing of grains. The successive steps are illustrated in figure 1. We have carried out 25 simulations with a ranging between 0.21 and 17 using between 1000 to 8000 grains.

3. Comments on the experimental results

Recent experiments by Lube *et al.* (2004) and Lajeunesse *et al.* (2004) have investigated the axisymmetric collapse of a column of grains onto a flat horizontal plane. The main result consists of scaling laws for the runout distance. Using the notation mentioned above (namely H_0 and R_0 are the initial height and radius of the column respectively, a the initial aspect ratio, and H_∞ and R_∞ respectively the height of the final deposit and the runout distance), Lube *et al.* (2004) find

$$\frac{R_\infty - R_0}{R_0} \simeq \begin{cases} 1.24\,a, & a \lesssim 1.7 \\ 1.6\,a^{1/2}, & a \gtrsim 1.7, \end{cases}$$

while Lajeunesse *et al.* (2004) find

$$\frac{R_\infty - R_0}{R_0} \simeq \begin{cases} 1.35\,a, & a \lesssim 0.74 \\ 2.0\,a^{1/2}, & a \gtrsim 0.74. \end{cases}$$

Moreover, quasi-two-dimensional experiments were carried out by Lube *et al.* (2005) by releasing granular columns confined between two vertical sidewalls. The following
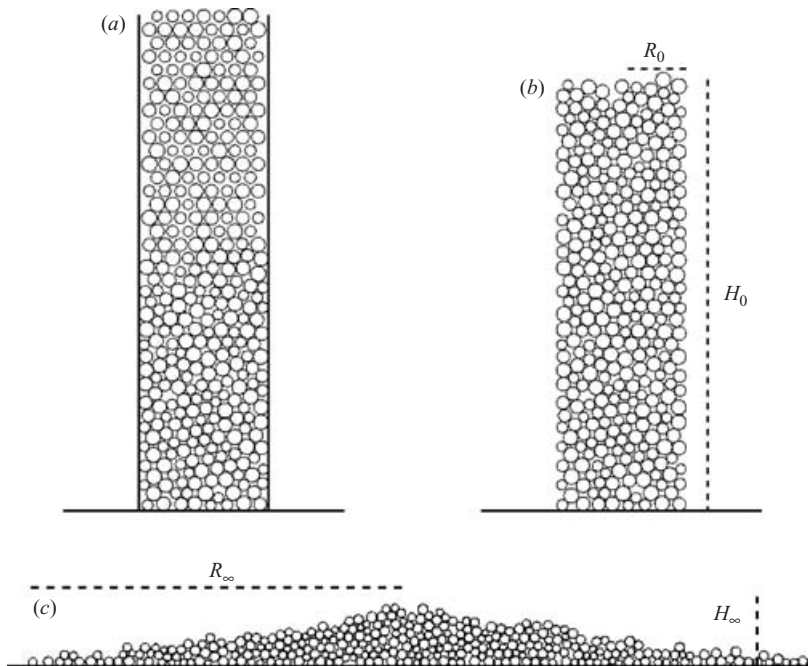
FIGURE 1. Preparation of a column of grains by a random rain of grains in the gravity field (*a*). The column is characterized by its initial radius R_0 and it initial height H_0 (*b*). After the collapse, the final deposit is characterized by the runout distance R_∞ and the height H_∞(*c*).

scalings were found:

$$\frac{R_\infty - R_0}{R_0} \simeq \begin{cases} 1.2\,a, & a \lesssim 2.3 \\ 1.9\,a^{2/3}, & a \gtrsim 2.3. \end{cases}$$

Quasi-two-dimensional experiments were also carried out by Balmforth & Kerswell (2005), where the influence of the gap between the two vertical walls confining the column collapse was also addressed. Their results indicate that the exponent of the power law depends on the size of the gap:

$$\frac{R_\infty - R_0}{R_0} \simeq \begin{cases} \lambda a^{0.65}, & \text{narrow gap} \\ \lambda a^{0.9}, & \text{large gap.} \end{cases}$$

In these experiments, the prefactor λ varies depending on the material used, whereas previous authors found a universal prefactor, perhaps due to a narrow range of experimental materials. However, scalings found for quasi-two-dimensional experiments in the narrow gap configuration give similar results for Lube *et al.* (2005) and Balmforth & Kerswell (2005), giving roughly $(R_\infty - R_0)/R_0 \propto a^{2/3}$. Zenit (2005) has reported results of numerical discrete simulations in which he finds similar values for the runout, but no clear transition in its behaviour depending on a.

The origin of the exponents is still under discussion. No model has yet achieved a comprehensive explanation of the collapse dynamics. In particular, a simple friction model cannot account for them. Supposing that the initial potential energy of the column is completely dissipated by the work of the friction forces along the runout distance leads to
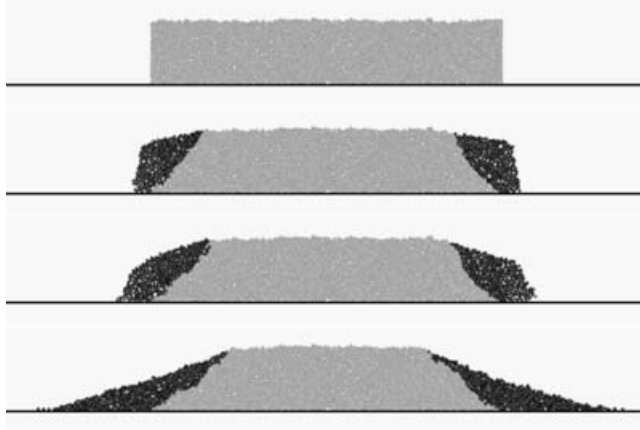
$$\mu_e m_0 g (R_\infty - R_0) = m_0 g H_0, \tag{3.1}$$

FIGURE 2. Grain movement in squat columns. The snapshots show successive times $t/T_\infty = 0$, 0.25, 0.37 and 1, where T_∞ is the duration of the collapse. The initial aspect ratio is $a = 0.37$. Shown in black are the grains with an accumulated horizontal displacement exceeding the mean grain diameter d. The scale in the four pictures is the same.

i.e.

$$\frac{(R_\infty - R_0)}{R_0} \propto a^1, \tag{3.2}$$

where m_0 is the total mass of grains, and μ_e is the effective coefficient of friction (constant by definition). The existence of different exponents in the experiments thus suggests that the dissipation process in the collapsing columns cannot be interpreted as a simple basal friction, and that the overall dynamics of the spreading must be more complex than usually postulated.

4. Scaling laws for the final deposit

4.1. *Qualitative description*

From a simple qualitative observation of the dynamics of the collapse, two different regimes can be distinguished depending on the value of the initial aspect ratio a. In the first regime, for small a, the flow simply consists of the fall of the edges of the initial column. The motion propagates from the edges inward, while a slope progressively builds up, along which the grains eventually stabilize. In this regime, only the grains situated at the sides of the columns fall, and as a result flow; by contrast, the grains situated inside the column have no motion and play no role at all in the spreading. This situation is illustrated in figure 2, where four successive snapshots of a collapsing pile with $a = 0.37$ are displayed. We have represented in black the grains with an accumulated horizontal displacement exceeding the mean grain diameter d. We observe that a majority of grains experience smaller displacement or none at all, and that most of the upper surface remains undisturbed.

The second regime, namely for high a, is radically different. In that case, the whole column falls in a vertical motion in response to gravity, causing most of the grains to take part in the dynamics. Four snapshots of the collapse of a column are shown in figure 3 for $a = 9.1$. Again, the black grains are those whose accumulated horizontal displacement exceeds d. Only a small fraction of grains situated in the centre of the
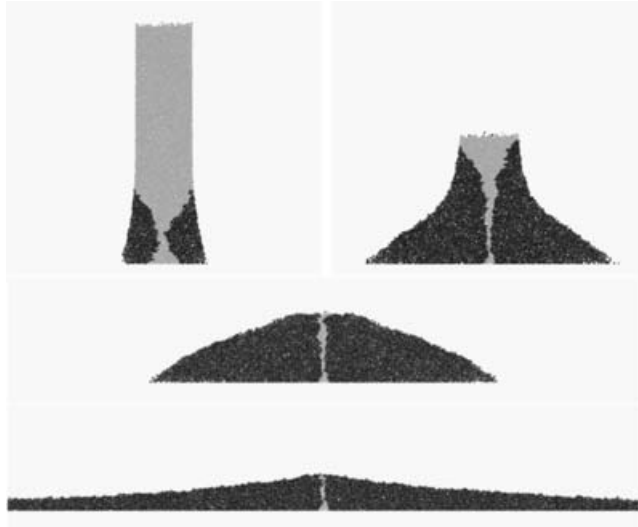
FIGURE 3. Grain movement in tall columns. The snapshots show successive times $t/T_\infty = 0.1$, 0.25, 0.37 and 1, where T_∞ is the duration of the collapse. The initial aspect ratio is $a = 9.1$. Shown in black are the grains with an accumulated horizontal displacement exceeding the mean grain diameter d. The scale in the four pictures is the same, and the deposit has been truncated in the last picture.

column remain undisturbed. When a tends to ∞, this fraction is expected to tend to zero.

An intermediate case between these two regimes is shown in figure 4, for $a = 0.9$; the entire upper surface is affected by the sideways flow, but a well-defined inner cone remains static. The shape of this inner cone is likely to be related to the frictional properties of the material, as suggested by Lajeunesse *et al.* (2004). In figure 5, final deposits are presented for columns with $a = 0.9$, 0.73, 0.55 and 0.37. To characterize better the properties of the granular packing, we include in the representation of the static inner cone the shear bands along which the flow develops. To do so, we no longer consider the grains which remain strictly static, but include also the grains which are involved in the shear dynamics. Hence, we represent in black grains with an accumulated horizontal displacement of more than $5d$. The slope of the cone obtained in this way gives the orientation of the shear bands, i.e. the orientation of the failure planes characterizing the flow of the edges. This allows an estimation of the frictional properties of the packing. We observe that the slope of the inner cone remains nearly constant, namely around $35°$, independently of a. It is tempting to assume that this slope reflects the mean frictional properties rather than the flow dynamics, and that the collapse, at least for small values of a, results from a Coulomb failure as suggested by Lajeunesse *et al.* (2004). In this case, assuming hydrostatic stress gives us an effective angle of internal friction $\varphi \simeq 20°$ for the packing of grains, equivalent to a coefficient of friction 0.36. We note that this value is different from the coefficient of friction acting at the contacts between grains, $\mu = 1$, and will also be different from the effective coefficient of basal friction evaluated later in §6. For greater values of a, the static inner cone is destroyed by the vertical dynamics of the upper grains and can no longer be observed in the final deposit.

The general observations on the shape of the collapsing columns described above are very close to previous experimental descriptions of the collapse.
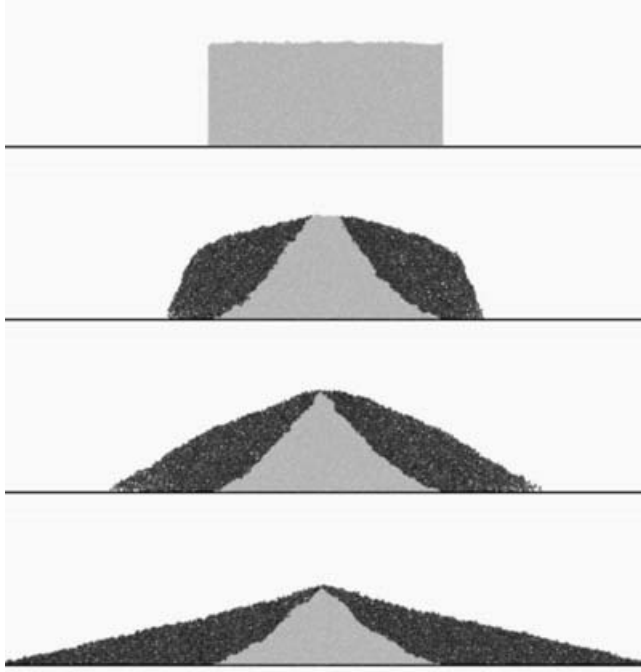
FIGURE 4. Grain movement in intermediate size columns. The snapshots show successive times $t/T_\infty = 0$, 0.25, 0.37 and 1, where T_∞ is the duration of the collapse. The aspect ratio is $a = 0.9$. Shown in black are the grains with an accumulated horizontal displacement exceeding the mean grain diameter d. The scale in the four pictures is the same.
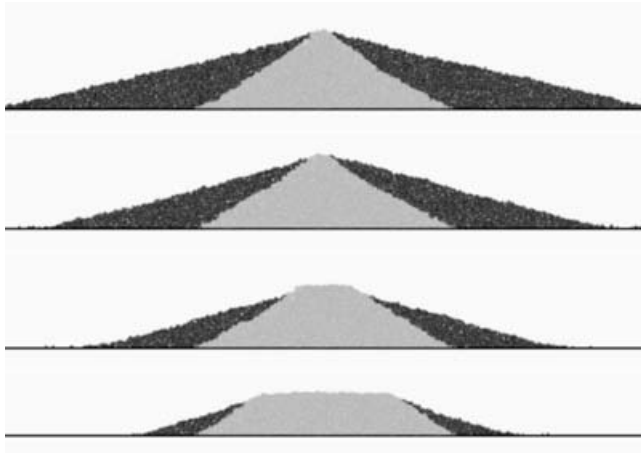

FIGURE 5. The inner static cone. Final deposits of columns with $a = 0.9$, 0.73, 0.55 and 0.37. The inner grey cone is the grains whose cumulated horizontal displacement is smaller than $5d$, and has a slope $\simeq 35°$ in all cases. The scale in the four pictures is the same.

4.2. Scaling laws for the final deposit

The shape of the final deposit resulting from the collapse and the spreading of the granular column is first characterized by the final runout distance R_∞. For each
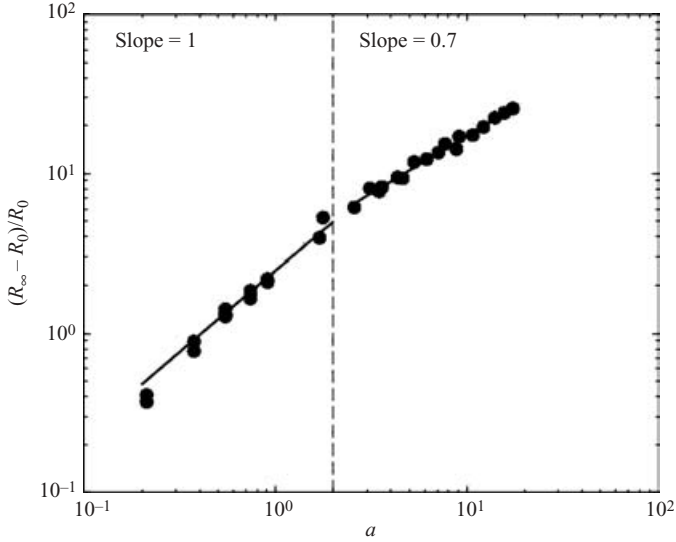
FIGURE 6. Final normalized runout distance $(R_\infty - R_0)/R_0$ as a function of the initial aspect ratio a.

experiment, R_∞ is evaluated from the position of the grains connected to the main mass by at least one contact. In other words, grains ejected from the flow, and undergoing a solitary trajectory independent of the collective behaviour of the flow, will not be taken into account. The reproducibility of the collapse is very good across independent realizations. The error when evaluating the runout is less than 3%. The final height of the central conical region H_∞ is also evaluated; it corresponds to the highest point of the deposit. We also evaluate the mean height of the deposit $\overline{H}_\infty$ from the total area covered by the grains; this is equivalent to a measure of the final potential energy of the deposit.

The evolution of the runout distance of the grains normalized by the initial radius of the column $(R_\infty - R_0)/R_0$ is plotted in figure 6 as a function of a. We observe the following dependence:

$$\frac{R_\infty - R_0}{R_0} \simeq \begin{cases} 2.5\,a, & a \lesssim 2 \\ 3.25\,a^\alpha, & a \gtrsim 2, \end{cases}$$

where $\alpha = 0.705 \pm 0.022$. As observed in laboratory experiments, the runout distance has two different behaviours depending on the value of a. For small values of a, a linear dependence is observed, while for larger a, the dependence is a power law. The scalings we obtain are in good agreement with the scalings observed from quasi-two-dimensional laboratory experiments, for which the exponent observed for sufficiently large a is 2/3 (Lube *et al.* 2005; Balmforth & Kerswell 2005), and the transition between the two behaviours occurs at $a = 2.3$ (Lube *et al.* 2005). The prefactors 2.5 and 3.25 obtained in the numerical simulations are higher than those observed experimentally by Lube *et al.* (2005), namely 1.2 and 1.9. This difference is very likely due to the respective frictional properties of the material; the circular shape of the numerical grains must enhance their mobility. Moreover, the dissipation induced by the friction with the two vertical walls confining the grains in the quasi-two-dimensional configuration, and the fact that the grains in a quasi-two-dimensional
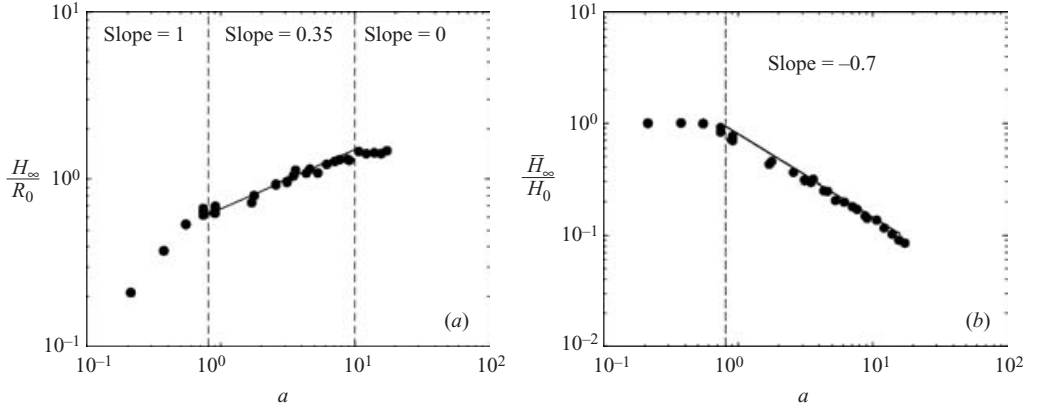
FIGURE 7. Final maximum height of the deposit normalized by the initial radius H_∞/R_0 (a), and mean height of the final deposit normalized by the initial height $\overline{H}_\infty/H_0$ (b) as functions of the initial aspect ratio a.

configuration are nevertheless arranged in a three-dimensional packing, are certain to affect the value of the prefactors.

The normalized final height H_∞/R_0 is plotted against a in figure 7; we observe

$$\frac{H_\infty}{R_0} \simeq \begin{cases} 1.0\,a, & a \lesssim 1 \\ 0.65\,a^{0.35}, & 1 \lesssim a \lesssim 10 \\ 1.45, & a \gtrsim 10. \end{cases}$$

The two-dimensional laboratory experiments show a similar behaviour, with an exponent 0.4 in Lube *et al.* (2005) and 0.5 in Balmforth & Kerswell (2005), but no transition is observed for $a \gtrsim 10$. Moreover, the behaviour observed in the case $a \lesssim 1$ is in agreement with the observations of Lajeunesse *et al.* (2004) in three-dimensional experiments.

The increase of the number of grains spreading sideways appears clearly when plotting the mean height of the deposit normalized by the initial height $\overline{H}_\infty/H_0$ against the initial aspect ratio a. From figure 7 the dependence is

$$\frac{\overline{H}_\infty}{H_0} \simeq \begin{cases} 1, & a \lesssim 0.8 \\ 0.8\,a^{-0.7}, & a \gtrsim 0.8, \end{cases}$$

as can be expected from the scaling of the runout distance and the mass conservation $R_\infty \overline{H}_\infty = R_0 H_0$. This relation shows the increasing transfer of potential energy to side-ways spreading motion and the decrease with a of the potential energy of the final deposit. As discussed in the introduction, these scaling laws are incompatible with a simple frictional behaviour, which would give $R_\infty/R_0 \propto a$ and $\overline{H}_\infty/R_0 \propto a^{-1}$. A first hypothesis is that the dynamics of the grains at the bottom of the column is responsible for a complex dissipation process dependent on the initial aspect ratio a. As a consequence, the energy available for spreading would also depend on a, and possibly cause the dependence of $(R_\infty - R_0)/R_0$ on a to be a power law. This aspect will be discussed further in §6.
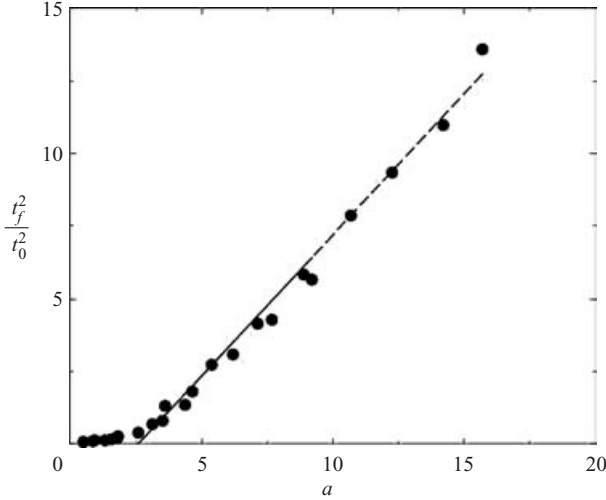
FIGURE 8. Dependence of $(t_f/t_0)^2$ on the initial aspect ratio a, where t_f is the time of free fall of the top of the column and $t_0 = (2R_0/g)^{1/2}$.

5. Dynamics of the collapse and spreading

5.1. *The vertical fall*

The dynamics of the collapse is first induced by the vertical fall of the grains. However, as stressed in §4.1, different behaviour can be observed depending on the value of a. Computing the position h of the top of the column over time, we are able to compare h with the free fall position given by $H_0 - 0.5gt^2$, and to evaluate the time t_f during which the top of the column is in free fall. The criterion used for the free fall to cease is $|h - (H_0 - 0.5gt^2)| > d$ (where d is the mean grain diameter). In figure 8 we have plotted $(t_f/t_0)^2$ as a function of the aspect ratio a, where $t_0 = (2R_0/g)^{1/2}$. For small values of a, the time of free fall t_f is nearly zero. However, as a increases, the following relation is satisfied:

$$\left(\frac{t_f}{t_0}\right)^2 \simeq 0.95a - 2.5,$$

i.e.

$$t_f \simeq \sqrt{\frac{2(H_0 - 2.5R_0)}{g}}.$$

This means that the top of the column undergoes free fall over a height $H_0 - 2.5R_0$. In other words, columns with $a \gtrsim 2.5$ have a period of free fall, while columns with $a \lesssim 2.5$ do not. We believe this transition in the vertical dynamics at $a \simeq 2.5$ to be at the origin of the transition observed in the scaling law for the runout distance in §4.2 and figure 6.

The fact that the top of the column is in free fall implies that the upper part of the column is not affected by the complex spreading process occurring at the bottom. As a consequence, two columns with the same initial radius R_0, but two different initial heights H_0^1 and H_0^2, should behave in the same way as long as the top of the smallest column remains above $\approx 2.5R_0$. The spreading at the base should not affect on the column above, and the top of the column should not see the spreading process

underneath. Once the limit height $2.5R_0$ is reached, the small column will rapidly spread out, while the taller column will accelerate further. This behaviour is clearly visible in the series of pictures shown in figure 9, representing the simultaneous collapse of two columns with heights H_0^1 and $H_0^2 \simeq 2H_0^1$ respectively, and same initial radius R_0. In the taller column, the grains initially situated above the height H_0^1 are represented in black to allow comparison of the two dynamics. From the beginning until $H_0^1 \simeq 2.5R_0$ (first four pairs of pictures), the top of the two columns remains undisturbed, and the spreading process occurring at their bases is identical. We then observe, in the respective evolution of the mass of grains initially situated under the height H_0^1 represented in grey, the effect of the fall of additional grains in black over the underlying deposit. In particular, the dynamics of pushing aside grains that would otherwise remain in the vicinity of the bottom of the column is obvious. Eventually, the black grains cover the underlying grey ones.

5.2. *The sideways propagation*

In the course of time, the sideways flow propagates outward; we denote by r the front position at any time t; eventually, r reaches the final value R_∞. The total duration of the collapse, until the sideways propagation stops and the whole deposit comes to rest, is denoted T_∞. In order to compare the dynamics of the spreading for different values of a, we plot on the same graph in figure 10 the evolution of the position of the front normalized by the final runout distance $(r - R_0)/(R_\infty - R_0)$ as a function of the time normalized by the total duration of the propagation t/T_∞, for $a = 0.9$, 1.8, 3.1, 7.7, 10.7 and 15.7. The plots collapse nicely onto a master curve, showing first a period of acceleration of the front, followed by a regime of constant propagation, and then a period of deceleration.

From the initial geometry of the column two characteristic times $t_0 = (2R_0/g)^{1/2}$ and $T_0 = (2H_0/g)^{1/2}$ can be formed, corresponding to the time of free fall over the distance R_0 and H_0 respectively. The collapse duration T_∞ is plotted against T_0 in figure 11. We observe a linear relation

$$T_\infty \simeq 2.25T_0 = 2.25 \left(\frac{2H_0}{g} \right)^{1/2},$$

implying that the duration of the experiment is controlled by the free fall of the column of initial height H_0. This is in agreement with experimental results, for which the duration of the experiments is found to be $\approx 3T_0$ (Lube *et al.* 2005).

However, although the time T_0 characterizes the spreading, it does not correctly capture the acceleration phase as can be seen in figure 12: the period of acceleration is well characterized by plotting, for different values of a, the normalized front position $(r - R_0)/R_0$ as a function of the normalized time t/t_0, instead of t/T_0. For high values of a, we clearly distinguish the acceleration phase followed by a constant velocity propagation phase. This evolution is not as obvious for small values of a, for which the deceleration phase occurs early and leaves less time for a constant velocity regime to establish. When plotting $(r - R_0)/R_0$ against a in a log-log representation, we see, up to $t/t_0 \simeq 1.5$, and for $a \gtrsim 1.8$, that the following relation fits:

$$\frac{r - R_0}{R_0} \simeq 0.68 \left(\frac{t}{t_0} \right)^2,$$

i.e.

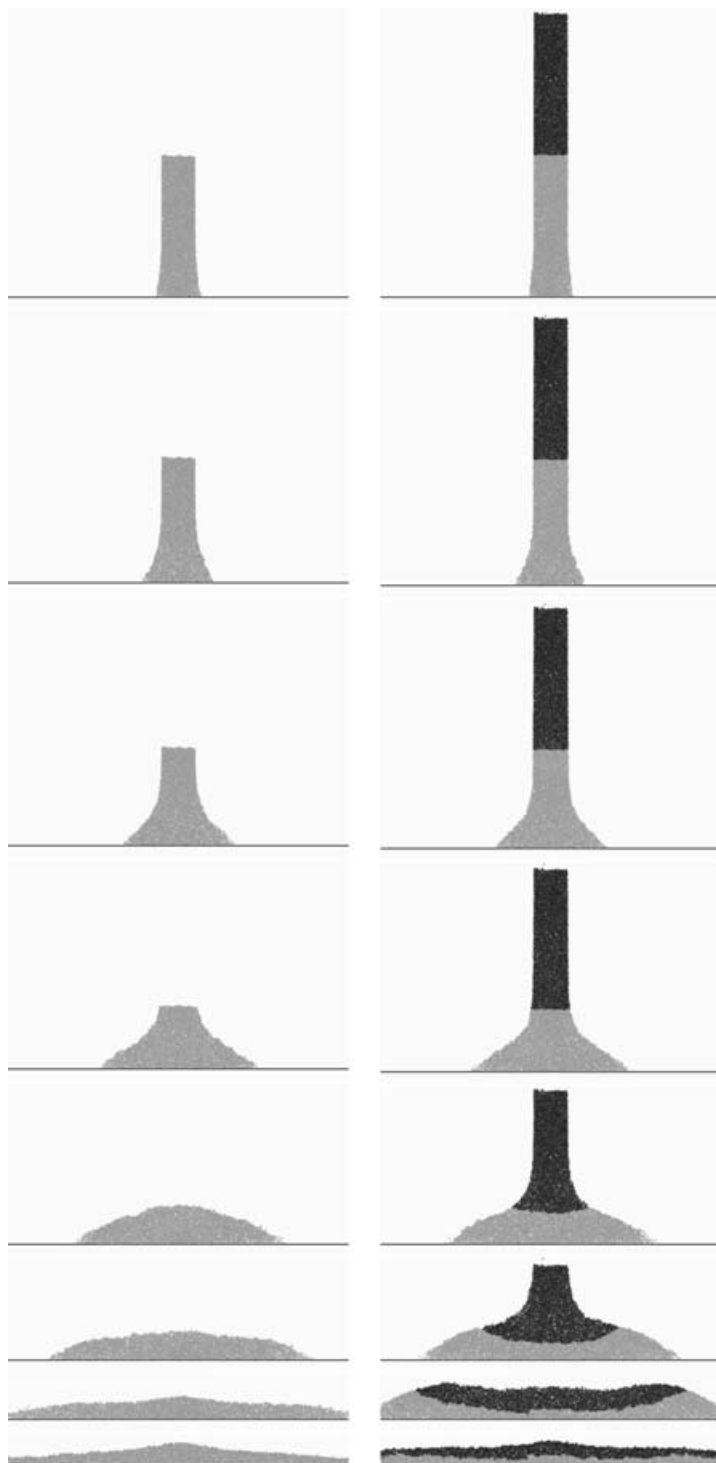$$r - R_0 \simeq 0.34gt^2.$$

FIGURE 9. Simultaneous collapse for $a = 8.8$ and $a = 17.4$. The upper pairs of pictures show the lack of dependence of the spreading on the height of the columns during the free fall. The lower pairs of pictures at later times show how the additional material in black pushes aside and eventually covers the underlying material in grey.
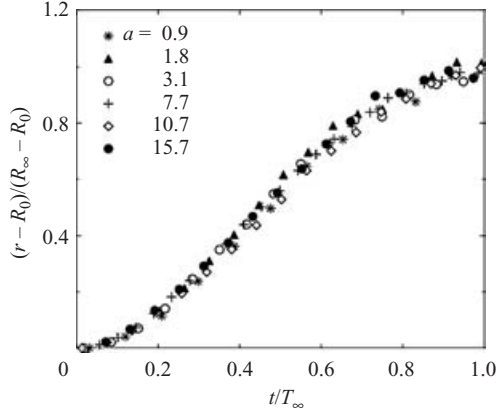
FIGURE 10. Position of the front normalized by the final runout distance, $(r - R_0)/(R_\infty - R_0)$, as a function of the time normalized by the total duration of the collapse, t/T_∞, for different values of a.
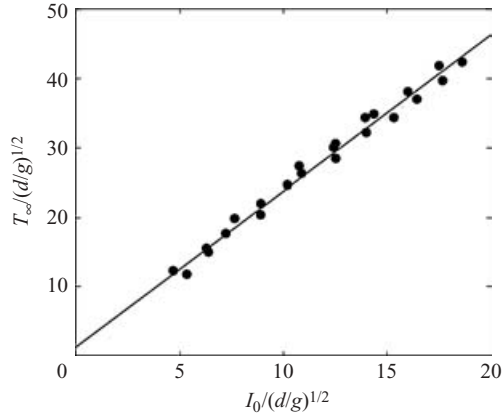

FIGURE 11. Total duration of the collapse T_∞ as a function of $T_0 = (2H_0/g)^{1/2}$ normalized by $(d/g)^{1/2}$. The linear relation is $T_\infty \simeq 2.25 T_0$.

Although this approximation is made over a very short time interval, it suggests that the onset of the spreading is driven by the free-fall dynamics. Where a constant velocity regime can be observed, the following relation is satisfied:

$$\frac{r - R_0}{R_0} \simeq 3\frac{t}{t_0} - 3,$$

which is equivalent to

$$r \simeq 1.5\, v_0 t, \quad r > 2R_0,$$

where $v_0 = (2gR_0)^{1/2}$ is the front propagation velocity, once a constant velocity regime is reached, after the front position has already run a distance $2R_0$.

Since the column is undergoing free fall for $a \gtrsim 2$, the accumulated mass of grains $m(t)$ expelled as a result of the collapse is given by $m(t) \propto \rho_s R_0 g t^2$, where ρ_s is the areal
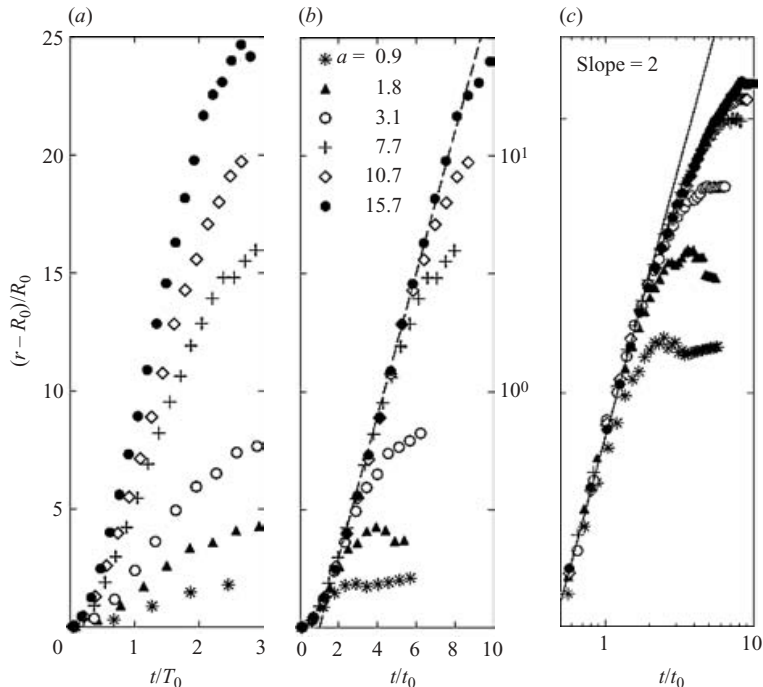
FIGURE 12. Position of the front normalized by the column initial radius $(r - R_0)/R_0$ for different values of a as a function of the normalized time t/T_0 in linear scale (*a*), and as a function of the normalized time t/t_0 in linear (*b*) and logarithmic (*c*) scales.

density of the grain packing. As the greater part of the front propagation involves a constant velocity, $r \propto v_0 t$, the increasing mass debit at the bottom of the column can only be accommodated by an increase of the height of the sideways flow. Moreover, the grains reaching the bottom, after they have been accelerated in the gravity field, have a greater momentum than the grains preceding them. This effect is responsible for the existence of a wave propagating outwards, transferring the mass from the centre towards the margin of the spreading for high values of a. An extreme case of this 'mass propagation' phenomenon is illustrated in figure 13 where the sideways flow is represented for $a = 70$.

This effect is more important in two-dimensional configurations than in axisymmetric ones, for which the increase of the surface area available for the spreading is quadratic with the front position, while the front propagation has been shown to obey the same behaviour $r \propto v_0 t$ (Lajeunesse *et al.* 2004). This suggests a purely geometrical explanation of the difference observed in the scaling laws between axisymmetric and two-dimensional experiments. Indeed, the typical front velocity $v_0 = (2gR_0)^{1/2}$, and the typical time of the experiment $T_0 = (2H_0/g)^{1/2}$, give for the runout distance the straightforward scaling law:

$$(R_\infty - R_0) = v_0 T_0 = (H_0 R_0)^{1/2},$$

corresponding to the observation $(R_\infty - R_0)/R_0 \simeq a^{1/2}$ in axisymmetric collapses. The difference with the two-dimensional case (namely $(R_\infty - R_0)/R_0 \simeq a^{2/3}$) could be due to
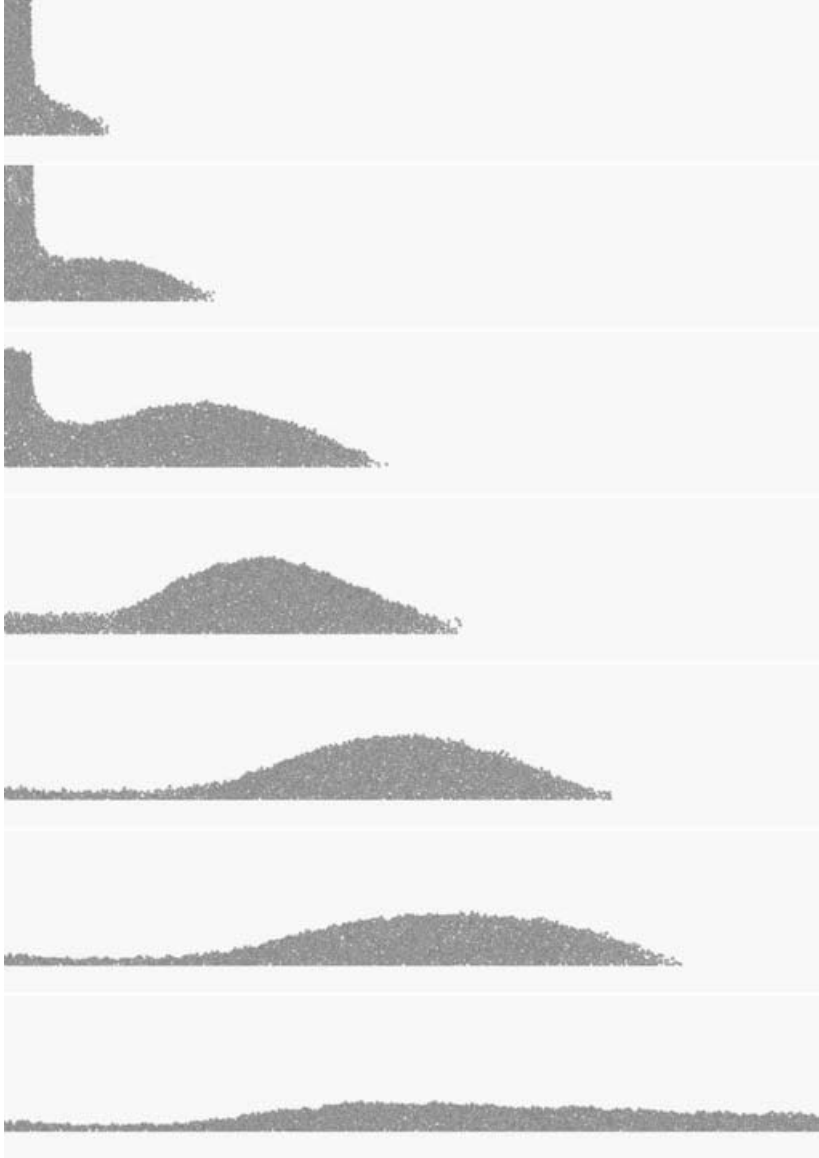
FIGURE 13. Successive snapshots of the spreading of a column with a very high aspect ratio $a = 70$. We observe the transfer of mass from the centre of the collapse towards the front of the flow. The scale is the same on all pictures.

the increase of mass in the sideways flow, whose effect would be to lengthen the deceleration phase. The contribution of the deceleration phase to the runout distance is not negligible in two-dimensions. Three examples of the contribution of the deceleration phase to the final runout distance are displayed in figure 14; up to one third of the total runout distance is achieved during the deceleration. This effect is presumably more important than in the axisymmetric configuration, for which the mass flux is more easily accommodated by the expanding surface area of the flow. This could also explain the difference of the exponents (1/2 in axisymmetric and 2/3 in
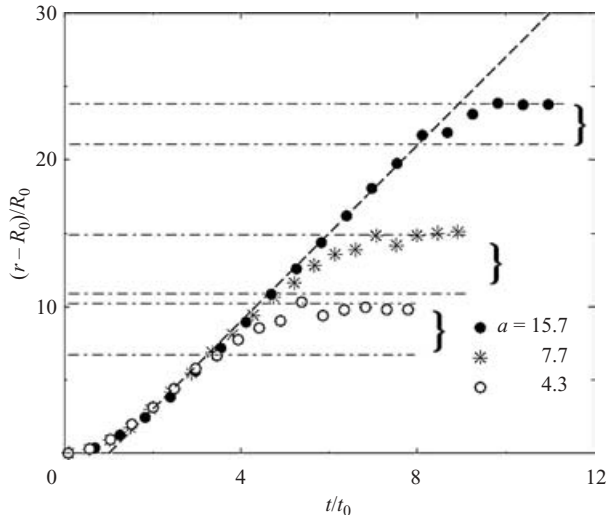
FIGURE 14. Position of the front normalized by the initial column radius $(r - R_0)/R_0$ as a function of the normalized time t/t_0 for different values of a. The linear evolution is stressed by the dashed line. Dashed-dotted lines indicate roughly the period of deceleration for each curve.

two-dimensions) in the scaling laws. A systematic analysis of the deceleration phase should help to solve this issue; however it is not undertaken in the present paper.

6. Energy transfer and dissipation

6.1. *Time evolution*

Basically, three successive stages can be identified in the history of a grain falling within the column. In a first stage, its initial potential energy is converted into vertical motion, and if the initial height of the grain allows for it, it will be accelerated down to the bottom. There, in a second stage, the grain will undergo collisions with the bottom plane or the surrounding grains, and its vertical motion will be converted into horizontal motion. In a third stage, the grain eventually leaves the base area of the column and flows sideways. Of course, this process involves collective dynamics of collisions and momentum lost and transfer, whose complexity makes the prediction of the trajectory of any grain difficult. For the same reason, a high initial potential energy is no guarantee, for a single individual grain, that it will travel a long way sideways. As an illustration of the complexity of the vertical to horizontal motion transfer, successive snapshots of the deformation of a collapsing column with $a \simeq 9.1$ are displayed in figure 15. The grains initially situated at the margins of the column, in the central area, and at the top, are represented in black. In the course of time, we observe that the grains travelling furthest are not those initially at the top. On the contrary, grains which started at a middle height or even lower finish nearer to the spreading front area. This behaviour is also visible in the deformation of the inner black slice.

The conversion of momentum from vertical to horizontal is likely to depend on the value of a. In figure 16, we have plotted for two collapsing columns with $a = 2.6$ and $a = 15.7$ the time evolution of the potential energy E_p, the vertical kinetic energy E_{k_y} and the horizontal kinetic energy E_{k_x} normalized by the initial potential energy
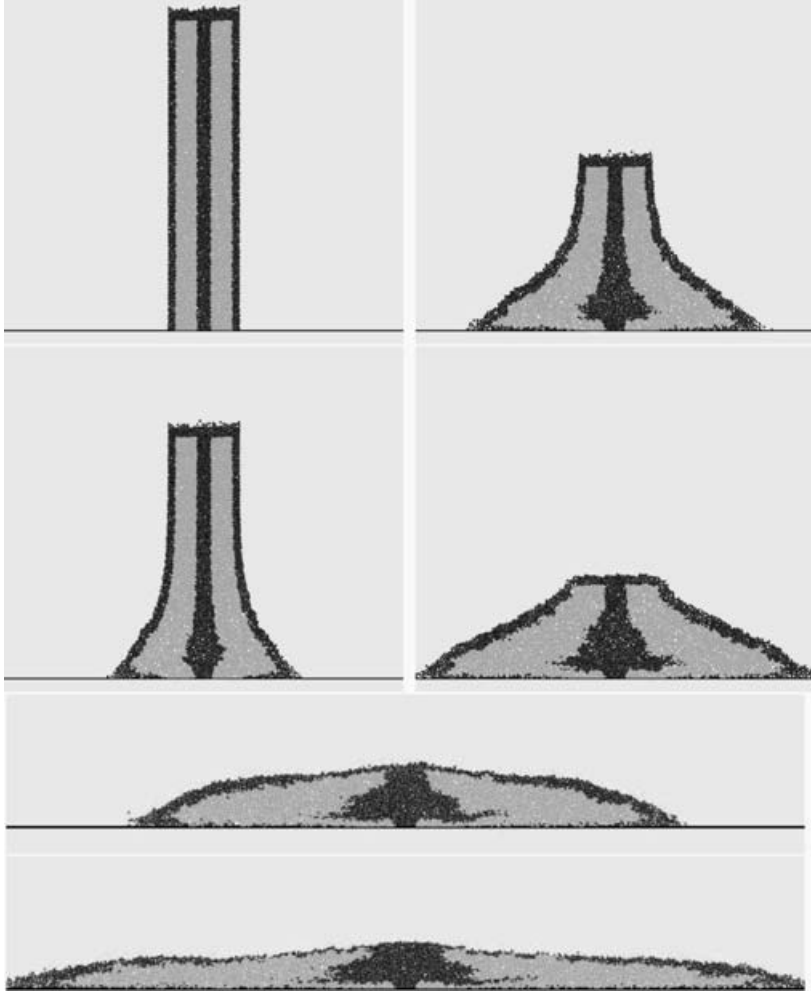
FIGURE 15. Deformation of a collapsing column with $a = 9.1$, at $t/T_\infty = 0, 0.2, 0.28, 0.35,$
0.45, and 0.75.

E_0, with

$$E_p = \sum_{p=1}^{N_p} m_p g h_p,$$

$$E_{k_i} = \frac{1}{2} \sum_{p=1}^{N_p} m_p v_{p,i}^2,$$

where $i = x$ or y, N_p is the total number of grains, m_p their mass, h_p their height and v_p their velocity. From these graphs we first see that a higher proportion of the initial energy is eventually dissipated by the column with $a = 15.7$, in agreement with the scaling of $\overline{H}_\infty/H_0$ in figure 7(b), which is equivalent to the ratio of the final potential energy to its initial value. Then, we observe that the conversion of energy from potential to kinetic in the vertical direction is much more efficient for $a = 15.7$. By contrast, a greater proportion of vertical kinetic energy is transferred into the
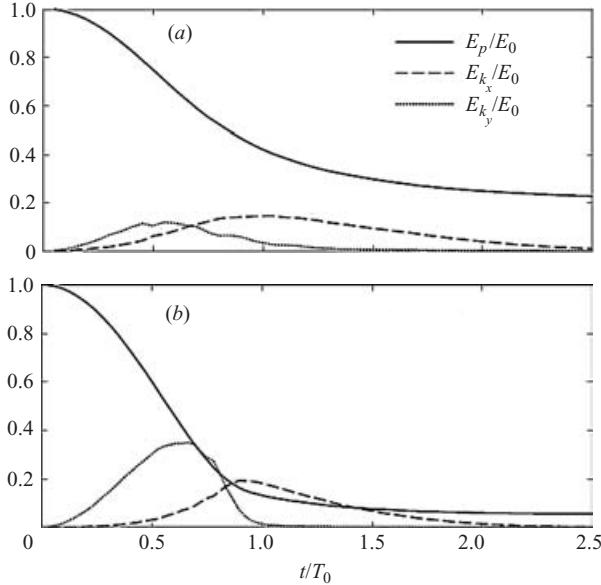
FIGURE 16. Time evolution of the potential energy E_p (continuous line), the vertical kinetic energy E_{k_y} (dotted line) and the horizontal kinetic energy E_{k_x} (dashed line) of the column for $a = 2.6$ (*a*) and $a = 15.7$ (*b*).

horizontal direction for $a = 2.6$. This suggests that the ability of the column to use its initial energy for spreading might depend on a.

6.2. *Conversion from potential to kinetic energy*

The total proportion of energy lost when the grains reach the bottom, and the conversion from vertical to horizontal momentum, are not obvious properties. Yet their role is fundamental in the spreading dynamics. Hence we define the vertical coefficient of restitution ρ_y (respectively the horizontal coefficient of restitution ρ_x) as the ratio of the total vertical (respectively horizontal) kinetic energy, averaged over the total duration of the collapse T_∞, to the initial potential energy E_0. These coefficients of restitution give an averaged picture of the energy dissipation over the whole collapse dynamics; by definition they do not capture the details of the highly unsteady and non-uniform dissipation process.

For each value of a, we thus compute the kinetic energy of the system averaged over the total duration of the collapse T_∞ in the vertical and horizontal direction:

$$\langle E_{k_i} \rangle = \frac{1}{T_\infty} \int_0^{T_\infty} \frac{1}{2} \sum_{p=1} N_p m_p v_{p,i}^2 \, \mathrm{d}t, \tag{6.1}$$

where $i = x$ or y.

For a theoretical comparison of the mean kinetic energy, we consider a partial column $kR_0 < y < H_0 - \frac{1}{2}gt^2$ in free fall at velocity gt during $T_f = (2(H_0 - kR_0)/g)^{1/2}$. Thus,

$$E_{k_y}^{thy} = \frac{1}{T_\infty} \int_0^{T_f} \frac{1}{2} \rho_s R_0 \left(H_0 - kR_0 - \frac{1}{2}gt^2 \right) g^2 t^2 \, \mathrm{d}t.$$

Setting $T_\infty = 2.25T_0$ with $T_0 = (2H_0/g)^{1/2}$ (see figure 11), and $E_0 = \frac{1}{2}\rho_s g R_0 H_0^2$ the initial
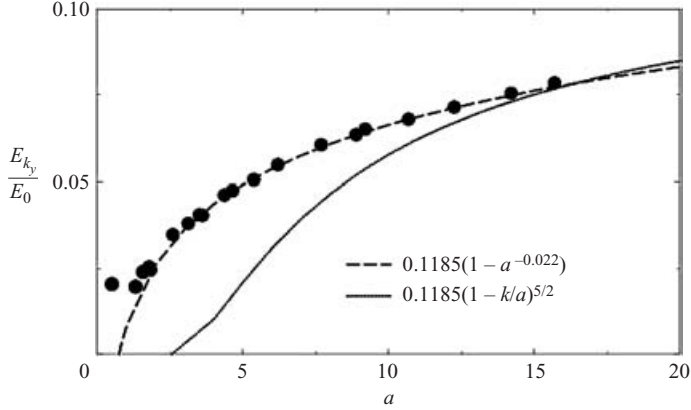
FIGURE 17. Vertical kinetic energy $\langle E_{k_y} \rangle$ averaged over the total duration of the collapse T_∞ and normalized by E_0, as a function of the initial aspect ratio a.

potential energy, we obtain

$$\frac{E_{k_y}^{thy}}{E_0} = 0.1185 \left(1 - \frac{k}{a} \right)^{5/2}. \tag{6.2}$$

From the analysis of the free fall in §5.1, we will use $k = 2.5$ in our comparison below. In other words, the above estimation of the energy holds for columns with aspect ratios $a > 2.5$ only.

We observe in figure 17 that over the range of aspect ratios studied, the numerical simulations have more vertical kinetic energy than our simple prediction (6.2). Equation (6.2) ignores any vertical motion below $y = kR_0$ and any motion after the free fall time T_f. Figure 17 suggests that at higher aspect ratios than those studied, our simple prediction may overestimate the mean vertical kinetic energy, which may be due to the grains not being in free-fall at height above $y = kR_0$. The results from the numerical simulations can be fitted empirically to

$$\frac{\langle E_{k_y} \rangle}{E_0} \simeq 0.1185(1 - a^{-0.022}). \tag{6.3}$$

The coefficient of restitution $\rho_y = \langle E_{k_y} \rangle / E_0$, characterizing the transfer of initial potential energy into vertical motion, is given by $\rho_y = 0.1185(1 - a^{-0.022})$, and is an increasing function of a. For $a \to \infty$, $\rho_y \to 0.1185$, meaning all the potential energy is converted into vertical motion following an ideal free fall. For intermediate values of a, potential energy conversion into vertical kinetic energy becomes more efficient with a. Similar behaviour in the dynamics of the sideways flow is discussed in the next section.

The mean horizontal kinetic energy $\langle E_{k_x} \rangle$, normalized by E_0, is plotted in figure 18 as a function of a. We observe

$$\frac{\langle E_{k_x} \rangle}{E_0} \simeq 0.16, \tag{6.4}$$

for $a \gtrsim 2.5$, which leads to a constant coefficient of restitution $\rho_x = \langle E_{k_x} \rangle / E_0 = 0.16$ characterizing the transfer of initial potential energy into horizontal motion in this range of aspect ratios. In other words, in spite of the complexity of the process taking place at the bottom of the column, the energy available for the horizontal motion is
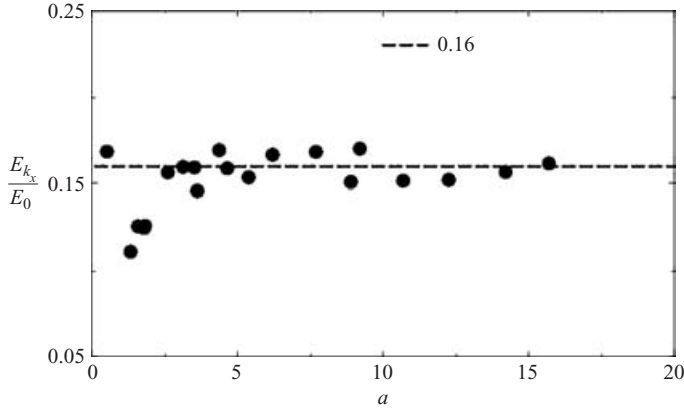
FIGURE 18. Horizontal kinetic energy $\langle E_{k_x} \rangle$ averaged over the total duration of the collapse T_∞ and normalized by E_0, as a function of the initial aspect ratio a.

simply proportional to the initial potential energy. Hence we can no longer suspect the dissipation process at the bottom of the column to be at the origin of the failure of the simple friction model described by equation (3.2). We have seen in §3 that the scaling laws imply that the relation $E_0 = \mu_e m_0 g R_\infty$ is not satisfied. Since $\langle E_{k_x} \rangle = \rho_x E_0$, we cannot have $\langle E_{k_x} \rangle = \mu_e m_0 g R_\infty$ either. This would indeed lead to $R_\infty = 0.16 H_0/\mu_e$, which is not observed. We may thus suppose that the assumption of a basal friction controlling the energy dissipation in the sideways flow is wrong. This question is tackled in the next subsection.

On computing the maximum kinetic energies in the vertical and horizontal directions during the collapse, the evolution of these two quantities as a function of a is found to be very similar to the evolution of the corresponding mean quantities in figures 17 and 18. The maximum values are about three times the mean values, as could be anticipated from the time evolution of E_{k_y} and E_{k_x} shown in figure 16. Characterizing the ability of the columns to convert vertical kinetic energy into horizontal kinetic energy by the ratio ρ_x/ρ_y, we obtain a decreasing function of the aspect ratio, suggesting the existence of a transient regime in the dynamics of spreading.

6.3. *Basal friction*

The basal friction is the dissipation mechanism most often postulated for dense flows of granular media, and has proven to be a reasonable description (Dade & Huppert 1998; Pouliquen 1999; Pouliquen & Forterre 2002). It implies the definition of an effective coefficient of friction μ_e, which is an average phenomenological representation of the more complex processes taking place at smaller scales through collisions and contact friction. In the case of the collapse of granular columns, the unsteady and non-uniform dynamics of the spreading makes any attempt to relate the value of the coefficient of friction to the properties of the flow difficult and uncertain. Hence, we define the effective coefficient of friction simply as the relationship between the energy dissipated and the distance run by the mass considered. We thus compare the energy made available for the flow with the work done by the mass of grains moving over the distance they eventually run. To do so, we define two vertical sections S situated at $-R_0$ and R_0, as shown in figure 19. Integrating over the total duration of the collapse T_∞, we compute the energy E_S crossing the sections S, and thus taking part in the flow, and the mass of grains m_S going through S. The energy E_S
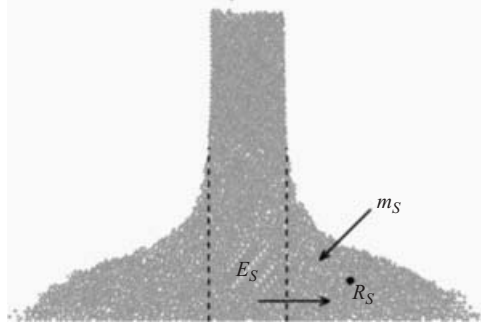
FIGURE 19. During the collapse, the energy E_S and the mass of grains m_S crossing the sections situated at $-R_0$ and R_0 are evaluated. The centre of mass of the sideways flow is at R_S.

is computed from both potential and kinetic energies of the grains. In the case of a simple effective friction process in the sideways flow, we should observe, independently of the dynamics occurring within the interval $[-R_0, R_0]$,

$$E_S = \mu_e m_S g(R_S - R_0),$$

where R_S is the position of the centre of mass of the mass m_S of grains in their final position, and μ_e is constant and independent of a.

The energy E_S normalized by the work $m_S g R_0$ of the moving mass m_S over a distance R_0 is plotted as a function of the non-dimensional flow distance $(R_S - R_0)/R_0$ in figure 20(a) for all the collapse experiments. We obtain a clear linear dependence establishing that energy dissipation is very well approximated by basal friction. The value of the effective coefficient of friction μ_e is given by the slope of the linear relation and is found to be $\mu_e \simeq 0.47$. If we assume that all the grains travel the final runout distance $R_\infty - R_0$, we again obtain a linear dependence, as seen in figure 20(b), but with a much smaller effective coefficient of friction $\mu_e \simeq 0.16$ expressing the maximum mobility of the flow. In all cases, the following relation is satisfied:

$$E_S = \mu_e m_S g(R_\infty - R_0). \tag{6.5}$$

In figure 21(a), the plot of E_S/E_0 as a function of a shows that as soon as $a \gtrsim 3$, $E_S/E_0 \simeq 0.44$. As could be inferred from the evolution of the mean horizontal energy (previous section), the energy available to the flow is simply proportional to the initial potential energy. The relation (6.5) can be rewritten

$$0.44 E_0 \simeq \mu_e m_S g(R_\infty - R_0), \tag{6.6}$$

or equivalently,

$$0.44 m_0 g H_0 \simeq \mu_e m_S g(R_\infty - R_0). \tag{6.7}$$

Finally, this leads to the following expression:

$$\frac{(R_\infty - R_0)}{R_0} \propto a \frac{m_0}{m_S}, \quad a \gtrsim 3.$$

This relation suggests that the disagreement between the scalings observed experimentally and the simple friction model (3.2) might rest in the definition of the mass of grains flowing sideways.

The normalized mass of grains crossing the section S and taking part in the sideways flow m_S/m_0 is plotted in figure 21(b) as a function of a. There exists a function
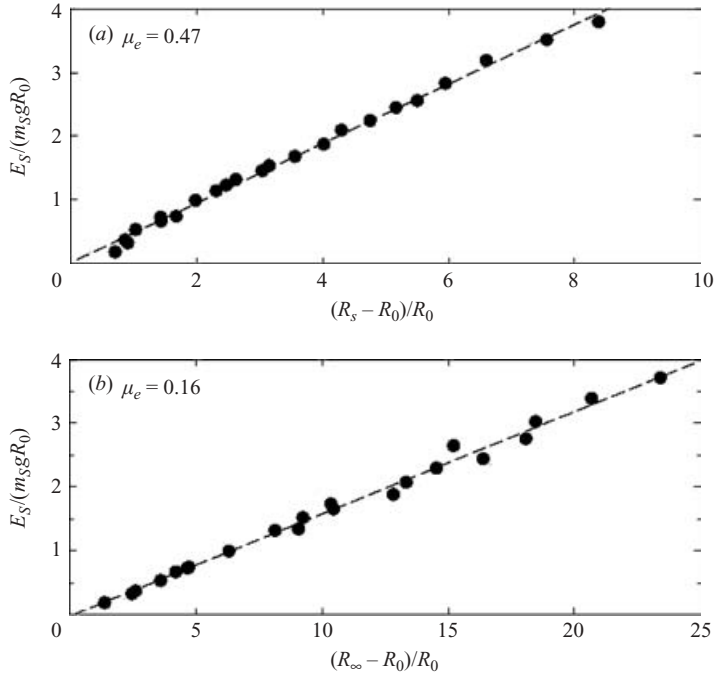
FIGURE 20. Energy available for the flow E_S normalized by the work $m_S g R_0$ of the mass m_S flowing over R_0 (a) as a function of the normalized distance moved by the centre of mass of the flowing grains $(R_S - R_0)/R_0$, and (b) as a function of the normalized runout distance of the flow $(R_\infty - R_0)/R_0$.
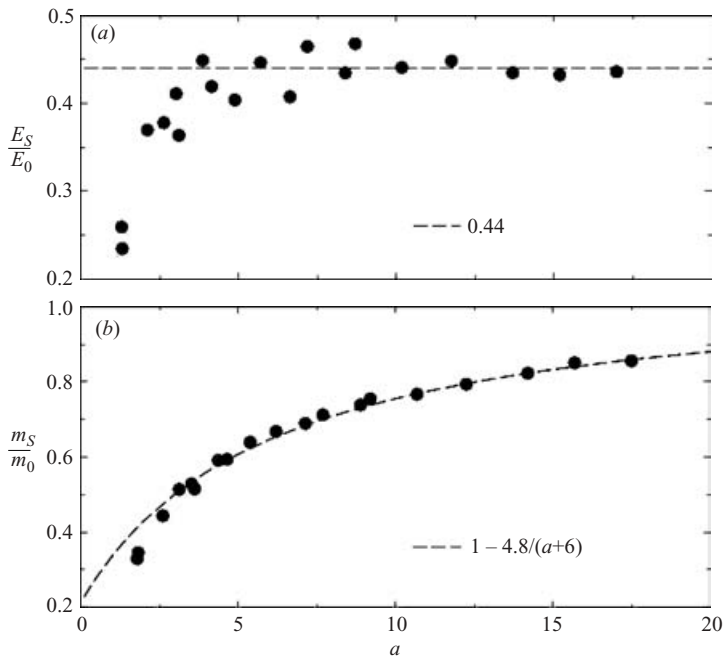

FIGURE 21. (a) Energy available for the flow E_S normalized by the initial potential energy E_0 as a function of a, and (b) mass of grains m_S taking part in the flow normalized by the initial total mass of grain m_0 as a function of a.

f of the aspect ratio such that

$$\frac{m_S}{m_0} \simeq 1 - f(a), \quad a \gtrsim 3, \tag{6.8}$$

with $f(a) \to 0$ when $a \to \infty$. No argument for the empirical fit $f(a) = 4.8/(a+6)$ is proposed; the main feature is that it captures a major aspect of the flow pheno-menology, the ejection of grains sideways. For small values of a, a small fraction of grains flows sideways, and most of the mass remains trapped in the interval $[-R_0, R_0]$ at the bottom of the initial column. In this range of aspect ratios, the fit (6.8) does not hold. However the fraction of grains flowing increases with a. When a becomes large, this fraction tends towards 1, as can be seen in figure 13 for $a = 70$. The increase of the proportion of mass taking part in the sideways flow might be related to the increase of mean vertical kinetic energy relatively to the initial energy. The increase of mass flowing sideways causes the friction dissipation process to be more efficient: as a increases, the same fraction of initial potential energy E_0 is driving more mass against friction. This additional dissipation may explain why an exponent lower than 1 appears in the scaling law.

This progressive increase of the mass flowing, bounded above by the initial mass m_0, also suggests that the dynamics of the collapse, in the range of a experimentally investigated, is transitional.

7. New scalings for a transient regime

In the range of aspect ratios a investigated in the present work, as well as in previous experimental work (Lube *et al.* 2004; Lajeunesse *et al.* 2004; Balmforth & Kerswell 2005), the collapses of the columns mainly differ in the mass of grains ejected sideways. The larger the initial aspect ratio a, the greater the proportion of grains ejected. Because of this difference, the propagating flows do not involve the same proportion of the initial mass of grains. For increasing values of a, the increase of mass will cause the work done by the flow to be more efficient, thus affecting the runout distance. However, the mass of grains flowing tends towards the initial mass m_0 when a increases, so we anticipate the dependence of the dissipation process on a ultimately to vanish. In this limit, the amount of energy dissipated by the flow would only depend on the runout distance. The dependence of the proportion of mass flowing sideways m_S/m_0 shown in figure 21(*b*) reflects this behaviour with an asymptotic evolution towards a new regime. On the basis of our observations of the phenomenology of the sideways flow, we thus suggest that there exists a function $f(a)$, satisfying $f(a) \to 0$ when $a \to \infty$, such as that

$$\frac{R_\infty - R_0}{R_0} \propto \frac{a}{(1 - f(a))}. \tag{7.1}$$

We present in figure 22 the variation of $(R_\infty - R_0)/R_0$ with a, the power-law approximation $3.25a^{0.7}$, and the empirical fit $a/(1 - f(a))$, where $f(a) = 4.8/(a+6)$ describes the mass ejection. We observe that in the range of aspect ratios investigated, the last choice is as acceptable as a power-law dependence.

The form of the function $f(a)$ will not be discussed at this stage. Basically, it represents the additional dissipation entailed in the increase of the proportion of mass flowing, while the proportion of energy available for the flow is constant, at least for $a \gtrsim 3$ in our simulations. The choice of an approximation of the form
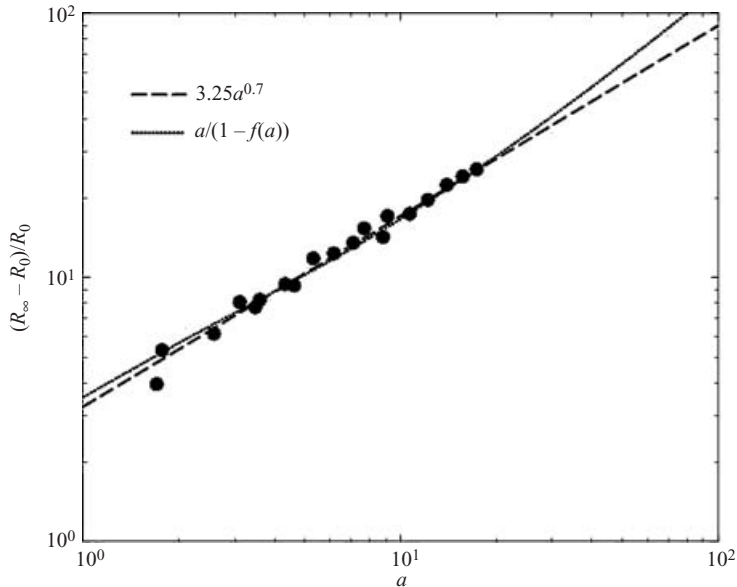
FIGURE 22. Final normalized runout distance $(R_\infty - R_0)/R_0$ as a function of a. Two different approximations are plotted: the power-law fit in the dashed line, and the function $a/(1 - f(a))$ in dotted line.

$a/(1 - f(a))$ for the runout distance has two implications:

(*a*) for large a, the runout distance should eventually increase like the height of the column, as expected by simple friction dynamics;

(*b*) it suggests that the power-law dependence might be fortuitous.

In the absence of a comprehensive model explaining either one or the other approximation, the proposition discussed here remains purely speculative. Moreover, subtle transitions in the behaviour of the columns for very large aspect ratios might occur which are difficult to predict. However, it matches the numerical results well, and provides a qualitative explanation for the nonlinear behaviour of the runout distance with a. Finally, it suggests that the key aspect of the collapse problem lies in the dynamics of ejection of the mass from the initial column itself, rather than in the characteristics of the sideways flow.

8. Summary and conclusion

We have numerically investigated the collapse and the spreading of two-dimensional columns of grains onto a horizontal plane using the Contact Dynamics method. This approach allows a detailed analysis of the dynamics of the collapse taking into account the energy and trajectory of the individual grains. Our results are generally in good agreement with previous experimental work carried out in quasi-two-dimensional configurations (Lube *et al.* 2005; Balmforth & Kerswell 2005). The collapse is first described in terms of the shape of the final deposit, and more specifically in terms of runout distance. A power-law dependence of the normalized runout distance on the initial aspect ratio of the columns is found for high aspect ratios, and a linear dependence for low aspect ratios. These scalings, experimentally observed by previous authors, are incompatible with a simple friction model of the collapse dynamics. We

show that the collapse is driven by a free fall of the column for sufficiently large aspect ratios. The existence, or absence, of free fall dynamics can explain the existence of two different scaling laws for the runout distance depending on the aspect ratio. The propagation of the front involves a constant velocity phase, followed by a deceleration phase which contributes significantly to the runout distance. An analysis of the mean kinetic energy of the grains shows that the dissipation occurring at the bottom of the column can be simply described by a constant coefficient of restitution. In particular, the energy avalaible for the sideways flow is simply proportional to the initial potential energy. A detailed analysis of the energy dissipated in the sideways flow and the work of the flowing mass clearly establishes that a constant basal friction is a good approximation of the dissipation process. Finally, we point to the dynamics of mass ejected sideways during the column collapse as playing a dominant role in the spreading dynamics, and as being responsible for the nonlinear behaviour of the normalized runout distance. This allows us to suggest that the scaling laws previously discussed for the runout distance are fortuitous, and should no longer apply when the aspect ratio increases. A new empirical fit is proposed, which is compatible with a friction model.

This conclusion has the following implications.

(*a*) Mass ejected sideways is a mechanism strongly dependent on the geometry of the collapse. In particular, we expect its effects to be more important in a two-dimensional configuration than in an axisymmetric collapse. This might be the origin of the difference is the scaling laws for the runout distance observed between two-dimensional (or quasi-two-dimensional) and axisymmetric configurations. In the limit of high aspect ratios however, the mass ejected tends towards the totality of the initial mass. In that limit, differences should no longer be observed between the two-dimensional and the axisymmetric configuration. In any case, our results suggest that an analytical expression for the runout distance should account for the process of the ejection of grains at the bottom of the collapsing column.

(*b*) The runout distance appears to be strongly dependent on the fall dynamics and not only on the effective flow properties, namely effective basal friction . Although high aspect ratios are difficult to find in nature, many rock falls or slope destabilizations involve a strong acceleration (and possibly free fall), which is a key aspect of the material ejection. From a geophysical perspective, this suggests that the mobility of a natural flow, usually defined as the ratio of the runout distance to the initial height of the material, is related to the early dynamics of the mass release as well as to the flowing properties of the material.

(*c*) Since the sideways flow undergoes a simple basal friction dissipation process, its modelling using shallow-water approaches is possible, but not straightforward. A difficulty lies in the description of the initial conditions represented by the vertical column collapse, which intrinsically violates the shallow-water assumptions. The issue is to achieve a correct description of the mass flux by limiting the energy released by the fall of the column. The column collapse, until now correctly reproduced only for low aspect ratios (Mangeney-Castelneau *et al.* 2004; Kerswell 2005), may also be recovered for large aspect ratios, provided the energy dissipation at the base of the column is correctly accounted for (Larrieu, Staron & Hinch 2006).

The influence of the material properties (inter-grain friction μ and restitution at collision ρ) on the overall dynamics of the collapse and the spreading will be the subject of further work.

H. Huppert. The first author thanks L. Duchemin for his unfailing avaibility for discussion.

REFERENCES

BALMFORTH, N. J. & KERSWELL, R. R. 2005 Granular collapse in two dimensions. *J. Fluid Mech.* **538**, 399–428.

CUNDALL, P. & STACK, O. 1979 *Geotechnique*, vol. **29** (1), pp. 47.

DADE, W. B. & HUPPERT, H. E. 1998 Long-runout rockfalls. *Geology* **26**, 803–806.

GOLDHIRSCH, I. 2003 Rapid granular flows. *Annu. Rev. Fluid Mech.* **35**, 267–293.

IVERSON, R. M., SCHILLING, S. P. & VALLANCE, J. W. 1998 Objective delineation of lahar-inundation hazard zones. *Geol. Soc. Am. Bull.* **110**, 972–984.

JEAN, M. 1994 Frictional contact in collections of rigid or deformable bodies: numerical simulation of geomaterial motions. In *Mechanics of Geomaterial Interfaces* (ed. A. P. S Selvadurai & M. J. Boulon), pp. 463–486. Elsevier.

KERSWELL R. R. 2005 Dam break with Coulomb friction: a model for granular slumping? *Phys. Fluids* **17**, 057101.

LAJEUNESSE, E., MANGENEY-CASTELNEAU, A. & VILOTTE, J.-P. 2004 Spreading of a granular mass on an horizontal plane. *Phys. Fluids* **16**, 2731–2381.

LARRIEU, E., STARON, L. & HINCH E. J. 2006 Raining into shallow water as a description of the collapse of a column of grains. To appear in *J. Fluid Mech. 50th Anniversary Edition.*

LUBE, G., HUPPERT, H. E., SPARKS, R. S. J. & HALLWORTH, M. A. 2004 Axisymmetric collapses of granular columns. *J. Fluid Mech.* **508**, 175–199.

LUBE, G., HUPPERT, H. E., SPARKS, R. S. J. & FREUNDT, A. 2005 Collapse of granular columns. *Phys. Rev.* E (submitted).

MANGENEY-CASTELNEAU, A., BOUCHUT, F., LAJEUNESSE, E., AUBERTIN, A., VILOTTE, J.-P. & PIRULLI, M. 2004 On the use of Saint-Venant equations for simulating the spreading of a granular mass. *J. Geophys. Res.* **199**, 177–215.

MOREAU, J.-J. 1994 Some numerical methods in multibody dynamics: Application to granular materials. *Eur. J. Mech.* A **4**, 93–114.

POULIQUEN, O. 1999 Scaling laws in granular flows down rough inclined planes. *Phys. Fluids* **11**, 542–548.

POULIQUEN, O. & FORTERRE, Y. 2002 Friction laws for dense granular flows: application to the motion of a mass down a rough inclined plane. *J. Fluid Mech.* **453**, 133–151.

RAJCHENBACH, J. 2000 Granular flows. *Adv. Phys.* **49**, 229–256.

SAVAGE, S. & HUTTER, K. 1989 The motion of a finite mass of granular material down a rough incline. *J. Fluid Mech.* **199**, 177–215.

ZENIT, R. 2005 Computer simulations of the collapse of a granular column. *Phys. Fluids* **17**, 031703.